Multiple-scattering theory for out-of-plane propagation of elastic waves in two-dimensional phononic crystals

Multiple-scattering theory for out-of-plane propagation of elastic waves in two-dimensional phononic crystals

Jun Mei, Zhengyou Liu[1] and Chunyin Qiu

Department of Physics, Wuhan University, Wuhan 430072, People's Republic of China

E-mail: zyliu@whu.edu.cn

Abstract
We extend the multiple-scattering theory (MST) to out-of-plane propagating elastic waves in 2D periodical composites by taking into account the full vector character. The formalism for both the band structure calculation and the reflection and transmission coefficient calculation for finite slabs is presented. The latter is based on a double-layer scheme, which obtains the reflection and transmission matrix elements for the multilayer slab from those of a single layer. Being more rapid in both the band structure and the transmission coefficient calculations for out-of-plane propagating elastic waves, our approach especially shows great advantages in handling the systems with mixed solid and fluid components, for which the conventional plane wave approach fails. As the applications of the formalism, we calculate the band structure as well as the transmission coefficients through finite slabs for systems with lead rods in an epoxy host, steel rods in a water host and water rods in a PMMA host.

1. Introduction

In recent years, there has been growing interest in classical wave propagation in periodic composite materials. The study of photonic crystals has taken the lead, with the theoretical prediction and experimental realization of photonic bandgaps [1, 2]. Recently, the focus has been extended to the study of acoustic and elastic waves in periodic composites termed phononic crystals [3–13].

In most theoretical and experimental studies of 2D phononic crystal, elastic waves have been assumed to propagate in the plane perpendicular to the cylinders, i.e., the wavevector has no component along the axis of the cylinders. Under such an assumption, the in-plane polarized and the out-of-plane polarized modes are decoupled. Of particular interest has been the search

---

[1] Author to whom any correspondence should be addressed.

for the absolute bandgap, defined as the gap common to both polarizations. For a 2D phononic crystal that displays an absolute bandgap for in-plane propagation, it might be of interest to know the extent to which the elastic waves can propagate out of plane while an absolute bandgap can still be seen in the corresponding band structure. The existence of such a gap would affirm the possibility of guiding elastic waves propagating perpendicularly to the plane of period, which not only constitutes the basis of many newly arisen research fields such as the acoustic-optical interaction in the photonic crystal fibres, but also has many important technological applications such as 'phononic crystal fibres' [11–13]. Another immediate application of this study concerns guiding the elastic waves in the plane of period when some defaults are added or dropped if the bandgap still exists even when the wavevector component along the cylinder's axis is not exactly zero.

In fact, there have been a few papers [11–13] involved in the band structure calculations for the out-of-plane propagating elastic waves in 2D phononic crystals by using the plane wave (PW) method [11, 12] or the finite element method (FEM) [13]. However, to the best of our knowledge, there is no publication about the transmission and reflection coefficient calculations for obliquely incident elastic waves in 2D finite slabs, which, however, makes up another very important aspect of theoretical investigation of phononic crystals. In addition, it is well known that for the band structure calculation the PW method [3–6, 11, 12] has a convergence problem when dealing with systems of either very high or very low filling ratios, or of large elastic mismatch. Meanwhile, the PW method cannot be used to calculate the transmittance and reflectance since it assumes either an infinite structure or periodic boundary conditions. The PW method is also less effective when dealing with disordered systems. On the other hand, although the FEM [13] is capable of dealing with the band structure calculation, it is also not applicable to the transmission coefficient calculation. In contrast, the multiple-scattering theory (MST) [7–10] has the fastest convergence speed in the band structure calculation for 2D or 3D phononic crystals composed of cylindrical or spherical objects for both ordered and disordered systems. At the same time, a layer MST theory [7] for 3D phononic crystals has also been successfully implemented, thus enabling rigorous calculation of the transmission and reflection coefficients for a slab of periodically arranged scatterers, and providing a direct way to compare theory with experiment. Furthermore, the special power of the MST approach consists in its ability in handling the phononic crystals with components of large elastic mismatch; a typical example is that of mixing solid and fluid components, for which the PW method has a convergence problem or completely fails.

In this paper, we present a rigorous multiple-scattering formalism for calculating both the band structure and the transmission coefficients for 2D elastic systems *when the wavevector has nonzero component along the normal of the periodic plane*. As the applications of the formalism, we perform the calculations for three 2D systems, including lead cylinders in epoxy, steel cylinders in water and water cylinders in PMMA matrix. The paper is organized as follows: the MST equations for the elastic waves in a 2D system are presented in section 2, and accordingly the 2D layer MST is presented in sections 3 and 4. Some numerical results and discussions are given in section 5, followed by a brief summary in section 6. Technical details of the theory are presented in the appendices.

2. Multiple-scattering theory for elastic waves

Multiple scattering of elastic waves by particles has been extensively studied during the last 20 years [7–10], and the scattering of *in-plane incident* elastic waves by a 2D periodic array of cylinders has also been studied very recently [8]. In this section, we present MST in its modern form for *obliquely incident* elastic waves scattered by a 2D periodic arrangement of

cylinders, and formulate the MST equations so that they are convenient to use in numerical calculations.

In a homogeneous medium, the elastic wave equation may be written as

$$(\lambda + 2\mu)\nabla(\nabla \cdot \vec{u}) - \mu\nabla \times \nabla \times \vec{u} + D\omega^2\vec{u} = 0, \tag{1}$$

where D is the density, and λ and μ are the Lamé constants of the medium. For an oblique incident elastic wave, the wavevector $\vec{k}$ has projections both on the plane of period i.e., the $x-y$ plane, and along the axis of the cylinders, i.e., the z axis. That is to say, $\vec{k} = \vec{k}_{xy} + k_z\hat{e}_z$, where $\vec{k}_{xy}$ is the projection on the $x-y$ plane and $k_z\hat{e}_z$ is the projection along the z axis. In the same way, the position vector $\vec{r}$ could also be decomposed into components parallel and perpendicular to the $x-y$ plane respectively: $\vec{r} = \vec{\rho} + z\hat{e}_z$, where $\vec{\rho}$ is the component parallel to the $x-y$ plane and $z\hat{e}_z$ is the component along the z axis. If we further define α and β as $\alpha^2 + k_z^2 = \frac{\omega^2 D}{\lambda + 2\mu}$ and $\beta^2 + k_z^2 = \frac{\omega^2 D}{\mu}$, respectively, then the general solution of equation (1) can be expressed as

$$\vec{u}(\vec{r}) = \sum_{n\sigma}[a_{n\sigma}\vec{J}_{n\sigma}(\vec{r}) + b_{n\sigma}\vec{H}_{n\sigma}(\vec{r})], \tag{2}$$

where $\vec{J}_{n\sigma}(\vec{r})$ and $\vec{H}_{n\sigma}(\vec{r})$ are, respectively, defined as

$$\begin{aligned}\vec{J}_{n1}(\vec{r}) &= \nabla[J_n(\alpha\rho)e^{in\phi}e^{ik_z z}] \\ \vec{J}_{n2}(\vec{r}) &= \nabla \times [\hat{e}_z J_n(\beta\rho)e^{in\phi}e^{ik_z z}] \\ \vec{J}_{n3}(\vec{r}) &= \frac{1}{\beta}\nabla \times \nabla \times [\hat{e}_z J_n(\beta\rho)e^{in\phi}e^{ik_z z}],\end{aligned} \tag{3}$$

and

$$\begin{aligned}\vec{H}_{n1}(\vec{r}) &= \nabla[H_n(\alpha\rho)e^{in\phi}e^{ik_z z}] \\ \vec{H}_{n2}(\vec{r}) &= \nabla \times [\hat{e}_z H_n(\beta\rho)e^{in\phi}e^{ik_z z}] \\ \vec{H}_{n3}(\vec{r}) &= \frac{1}{\beta}\nabla \times \nabla \times [\hat{e}_z H_n(\beta\rho)e^{in\phi}e^{ik_z z}],\end{aligned} \tag{4}$$

where $J_n(x)$ is the cylindrical Bessel function and $H_n(x)$ is the Hankle function of the first kind. In equation (2), the index σ, ranging from 1 to 3, stands for three kinds of modes: $\sigma = 1$ is for the longitudinal modes, and $\sigma = 2, 3$ represent the two transverse modes. When the coefficients $b_{n\sigma}$ are zero, $\vec{u}(\vec{r})$ represents the incoming wave, and $a_{n\sigma} = 0$ implies that $\vec{u}(\vec{r})$ consists of only the outgoing wave. In a composite medium, the displacement in each homogeneous region obeys equation (1), and thus can be expressed in the form of equation (2). By regarding the composite medium as composed of a host matrix and embedded scatterers, the incident wave for scatterers i may be expressed as

$$\vec{u}_i^{in}(\vec{r}_i) = \sum_{n\sigma} a_{n\sigma}^i \vec{J}_{n\sigma}^i(\vec{r}_i), \tag{5}$$

where $\vec{r}_i$ is measured from the centre of scatterer i. The wave scattered by scatterer i may be expressed as

$$\vec{u}_i^{sc}(\vec{r}_i) = \sum_{n\sigma} b_{n\sigma}^i \vec{H}_{n\sigma}^i(\vec{r}_i). \tag{6}$$

According to MST, the wave incident on a given scatterer consists of two parts. One is the externally incident wave $\vec{u}_i^{in(0)}(\vec{r}_i)$, which may be expanded as

$$\vec{u}_i^{in(0)}(\vec{r}_i) = \sum_{n\sigma} a_{n\sigma}^{i(0)} \vec{J}_{n\sigma}^i(\vec{r}_i). \tag{7}$$

The second part is the sum of all the scattered waves except those from scatterer i, given by

$$\vec{u}_i^{\text{in}}(\vec{r}_i) - \vec{u}_i^{\text{in}(0)}(\vec{r}_i) = \sum_{j \neq i} \sum_{n''\sigma''} b_{n''\sigma''}^j \vec{H}_{n''\sigma''}^j(\vec{r}_j), \tag{8}$$

where $\vec{r}_i$ and $\vec{r}_j$ refer to the position of the same spatial point measured from scatterer i and j, respectively. With $\vec{R}_{i(j)}$ denoting the position of scatterer $i(j)$, we have $\vec{r}_j = \vec{r}_i - (\vec{R}_j - \vec{R}_i)$. It may be proved that (see appendix A for details)

$$\vec{H}_{n''\sigma''}^j(\vec{r}_i - (\vec{R}_j - \vec{R}_i)) = \sum_{n\sigma} G_{n''\sigma''n\sigma}(\vec{R}_j - \vec{R}_i) \vec{J}_{n\sigma}^i(\vec{r}_i), \tag{9}$$

where G is the so-called vector structure constant, and is given by

$$G_{n\sigma n'\sigma'}(\vec{R}) = \begin{cases} X_{nn'}^\alpha(\vec{R}) & \sigma = \sigma' = 1 \\ X_{nn'}^\beta(\vec{R}) & \sigma = \sigma' = 2, \quad \sigma = \sigma' = 3, \end{cases} \tag{10}$$

and $X_{nn'}^\kappa(\vec{R})$ is the so-called structure constants for scalar waves, defined as

$$X_{nn'}^\kappa(\vec{R}) = H_{n'-n}(\kappa R)\text{e}^{-\text{i}(n'-n)\phi_R}, \tag{11}$$

where $\kappa = \alpha, \beta$ and ϕ_R is the argument of $\vec{R}$. By defining $G_{n''\sigma''n\sigma}^{ij} = G_{n''\sigma''n\sigma}(\vec{R}_j - \vec{R}_i)$, $\vec{H}_{n''\sigma''}^j(\vec{r}_j)$ may be expressed as

$$\vec{H}_{n''\sigma''}^j(\vec{r}_j) = \sum_{n\sigma} G_{n''\sigma''n\sigma}^{ij} \vec{J}_{n\sigma}^i(\vec{r}_i). \tag{12}$$

For a given scatterer, the scattered displacement field is completely determined from the incident field through the scattering matrix. There is a relation between the expansion coefficients $A = \{a_{n\sigma}^j\}$ and $B = \{b_{n\sigma}^j\}$:

$$b_{n''\sigma''}^j = \sum_{n'\sigma'} t_{n''\sigma''n'\sigma'}^j a_{n'\sigma'}^j, \tag{13}$$

where the scattering matrix $T = \{t_{n\sigma n'\sigma'}\}$ can be obtained from the elastic Mie scattering solution of a scatterer. Substituting equations (5), (7), (12) and (13) into equation (8), we arrive at

$$\sum_{jn'\sigma'} [\delta_{ij}\delta_{nn'}\delta_{\sigma\sigma'} - \sum_{n''\sigma''} t_{n''\sigma''n'\sigma'}^j G_{n''\sigma''n\sigma}^{ij}] a_{n'\sigma'}^j = a_{n\sigma}^{i(0)}. \tag{14}$$

This is the final equation for a multiple-scattering system. It has the general form of the scalar KKR theory. For a finite and/or disordered system, we must solve this equation in order to investigate the system response to external perturbations. The normal modes of the system may be obtained by solving the following secular equation, in the absence of an external incident wave:

$$\det \left| \delta_{ij}\delta_{nn'}\delta_{\sigma\sigma'} - \sum_{n''\sigma''} t_{n''\sigma''n'\sigma'}^j G_{n''\sigma''n\sigma}^{ij} \right| = 0. \tag{15}$$

For a periodic system, equation (15) may be transformed to

$$\det \left| \delta_{ss'}\delta_{nn'}\delta_{\sigma\sigma'} - \sum_{n''\sigma''} t_{n''\sigma''n'\sigma'}^{s'} G_{n''\sigma''n\sigma}^{ss'}(\vec{k}) \right| = 0, \tag{16}$$

where s and s' label the scatterers in the unit cell with position vector $\vec{o}_s$ and $\vec{o}_{s'}$, and $G_{n''\sigma''n\sigma}^{ss'}(\vec{k})$ is defined as

$$G_{n''\sigma''n\sigma}^{ss'}(\vec{k}) = \sum_{\vec{R}} G_{n''\sigma''n\sigma}(\vec{o}_{s'} - \vec{o}_s - \vec{R}) \exp(\text{i}\vec{k} \cdot \vec{R}), \tag{17}$$

where the sum $\sum_{\vec{R}}$ is over all lattice sites. The solution of equation (16) gives the band structure of an elastic periodic system.
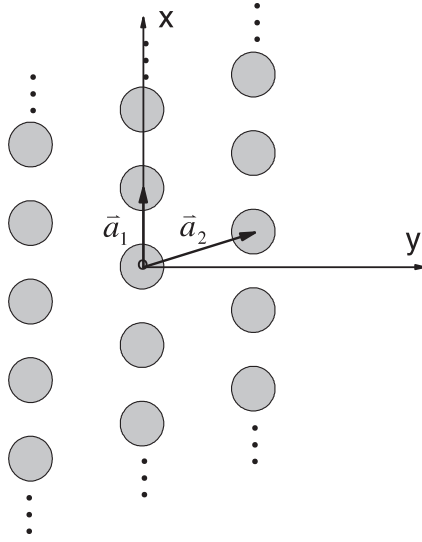
Figure 1. 2D phononic crystal consisting of a sequence of identical monolayers, with $\vec{a}_1$ and $\vec{a}_2$ being primitive vectors.

(This figure is in colour only in the electronic version)

3. Elastic wave scattering by a planar layer of scatterers

The study of elastic wave scattering by a periodic array of scatterers has a long history. In this section and the next, we formulate MST in a layer-by-layer approach for calculating the transmission and reflection from a finite slab of periodically arranged scatterers. We assume that a layer of cylinder scatterers are located periodically on sites $\vec{R}_n$ of a 1D lattice along the x axis, where $\vec{R}_n = n\vec{a}_1$, with n being integer and $\vec{a}_1$ being the primitive vector along the x axis. The y axis is assumed to point to the right of the x–z plane (as shown in figure 1).

A plane elastic wave obliquely incident on the cylinders may be expressed in general as

$$\vec{u}_\alpha^{\text{in}\pm}(\vec{r}) = \sum_g \vec{u}_{\alpha g}^{\text{in}\pm}(\vec{r}) = \sum_g \vec{V}_{\alpha g}^{\text{in}\pm} \exp(i\vec{k}_{\alpha g}^\pm \cdot \vec{\rho}) \exp(ik_z z),$$

$$\vec{V}_{\alpha g}^{\text{in}\pm} \times (\vec{k}_{\alpha g}^\pm + k_z \hat{e}_z) = 0,$$

$$\vec{u}_\beta^{\text{in}\pm}(\vec{r}) = \sum_g \vec{u}_{\beta g}^{\text{in}\pm}(\vec{r}) = \sum_g \vec{V}_{\beta g}^{\text{in}\pm} \exp(i\vec{k}_{\beta g}^\pm \cdot \vec{\rho}) \exp(ik_z z),$$

$$\vec{V}_{\beta g}^{\text{in}\pm} \cdot (\vec{k}_{\beta g}^\pm + k_z \hat{e}_z) = 0,$$

(18)

$$\vec{k}_{\alpha g}^\pm = \left(\vec{k}_\parallel + \vec{g}, \pm\sqrt{\alpha^2 - |\vec{k}_\parallel + \vec{g}|^2} \right),$$

$$\vec{k}_{\beta g}^\pm = \left(\vec{k}_\parallel + \vec{g}, \pm\sqrt{\beta^2 - |\vec{k}_\parallel + \vec{g}|^2} \right),$$

(19)

where $\vec{u}_\alpha^{\text{in}\pm}(\vec{r})$ and $\vec{u}_\beta^{\text{in}\pm}(\vec{\rho})$ represent the longitudinal and transverse plane elastic waves, respectively, the sign + means incident from the left of the plane (incident along positive y), and − means incident from the right of the plane (incident along negative y). Here, $\vec{g} = n\frac{2\pi}{a_1}\hat{e}_x$ is one of the 1D reciprocal lattice vectors along the x axis. Thus, the incident plane elastic waves may be expressed as

$$\vec{u}^{\text{in}}(\vec{r}) = \vec{u}_\alpha^{\text{in}}(\vec{r}) + \vec{u}_\beta^{\text{in}}(\vec{r}) = \sum_{sg} \vec{u}_{\alpha g}^{\text{ins}}(\vec{r}) + \sum_{sg} \vec{u}_{\beta g}^{\text{ins}}(\vec{r}).$$

(20)

The incident elastic waves can also be expanded in the cylinder coordinate basis:

$$\vec{u}^{\text{in}}(\vec{r}) = \sum_{n\sigma} a_{n\sigma} \vec{J}_{n\sigma}(\vec{r}), \tag{21}$$

or, more explicitly,

$$\vec{u}^{\text{in}}_{\alpha}(\vec{r}) = \sum_{n} a_{n1} \vec{J}_{n1}(\vec{r}),$$
$$\vec{u}^{\text{in}}_{\beta}(\vec{r}) = \sum_{n} a_{n2} \vec{J}_{n2}(\vec{r}) + \sum_{n} a_{n3} \vec{J}_{n3}(\vec{r}), \tag{22}$$

where the coefficients $a_{n\sigma}$ derived from $\vec{V}^{\text{in}\pm}_{\alpha g}$ and $\vec{V}^{\text{in}\pm}_{\beta g}$ (see appendix B for the details), may be expressed as

$$a_{n1} = \sum_{sg} \vec{V}^{\text{ins}}_{\alpha g} \cdot A^{gs}_{n1},$$
$$a_{n2} = \sum_{sg} \vec{V}^{\text{ins}}_{\beta g} \cdot A^{gs}_{n2}, \tag{23}$$
$$a_{n3} = \sum_{sg} \vec{V}^{\text{ins}}_{\beta g} \cdot A^{gs}_{n3},$$

with $\vec{A}^{gs}_{n\sigma}$ defined as

$$\vec{A}^{gs}_{n1} = \frac{\text{i}^{n-1}}{\alpha^2 + k_z^2} \exp(-\text{i}n\phi^s_{\vec{k}\alpha g})(\vec{k}^s_{\alpha g} + k_z \hat{e}_z),$$
$$\vec{A}^{gs}_{n2} = \frac{\text{i}^{n-1}}{\beta^2} \exp(-\text{i}n\phi^s_{\vec{k}\beta g})(\vec{k}^s_{\beta g} \times \hat{e}_z), \tag{24}$$
$$\vec{A}^{gs}_{n3} = \frac{\text{i}^{n}}{\beta^2 + k_z^2} \exp(-\text{i}n\phi^s_{\vec{k}\beta g})\left(-\frac{k_z}{\beta}\vec{k}^s_{\beta g} + \beta\hat{e}_z\right).$$

In general, the wave scattered by a scatterer i may be expanded as $\sum_{n\sigma} b^i_{n\sigma} \vec{H}^i_{n\sigma}(\vec{r}_i)$, which is completely determined by the incident waves plus the scatterer parameters and geometry. The total scattered wave contains contributions from all the scatterers in the plane:

$$\vec{u}^{\text{sc}}(\vec{r}) = \sum_{in\sigma} b^i_{n\sigma} \vec{H}^i_{n\sigma}(\vec{r}_i). \tag{25}$$

According to the Bloch theorem, we have

$$\vec{u}^{\text{sc}}(\vec{r}) = \sum_{n\sigma} b_{n\sigma} \sum_{\vec{R}} \exp(\text{i}\vec{k}_{\parallel} \cdot \vec{R}) \vec{H}_{n\sigma}(\vec{r} - \vec{R}) \tag{26}$$

where $\{b_{n\sigma}\}$ are the expansion coefficients (defined above) for the central scatterer, with the superscript omitted. It may be proved (see appendix C for the details) that $B = ZA$,

$$Z = [I - TG^{\text{Tr}}(\vec{k}_{\parallel})]^{-1}T, \tag{27}$$

where $A = \{a_{n\sigma}\}$, $B = \{b_{n\sigma}\}$, $T = \{t_{n\sigma n'\sigma'}\}$ is the scattering matrix for a single scatterer, and $G = \{G_{n\sigma n'\sigma'}(\vec{k}_{\parallel})\}$ with

$$G_{n\sigma n'\sigma'}(\vec{k}_{\parallel}) = \sum_{\vec{R}}{}' \exp(\text{i}\vec{k}_{\parallel} \cdot \vec{R}) G_{n\sigma n'\sigma'}(-\vec{R}). \tag{28}$$

Here the sum over $\vec{R}$ covers the whole two-dimensional lattice, excluding $\vec{R} = 0$. We use the method presented in [14] to evaluate the sum in equation (28). The superscript Tr of G in equation (27) denotes transposition.

It can be shown (see appendix D for details) that

$$\sum_{\vec{R}} \exp(i\vec{k}_{\parallel} \cdot \vec{R}) \vec{H}_{n1}(\vec{r} - \vec{R}) = \sum_{g} \vec{B}_{n1}^{g\pm} \exp(i\vec{k}_{\alpha g}^{\pm} \cdot \vec{\rho}) \exp(ik_z z),$$

$$\sum_{\vec{R}} \exp(i\vec{k}_{\parallel} \cdot \vec{R}) \vec{H}_{n2}(\vec{r} - \vec{R}) = \sum_{g} \vec{B}_{n2}^{g\pm} \exp(i\vec{k}_{\beta g}^{\pm} \cdot \vec{\rho}) \exp(ik_z z), \quad (29)$$

$$\sum_{\vec{R}} \exp(i\vec{k}_{\parallel} \cdot \vec{R}) \vec{H}_{n3}(\vec{r} - \vec{R}) = \sum_{g} \vec{B}_{n3}^{g\pm} \exp(i\vec{k}_{\beta g}^{\pm} \cdot \vec{\rho}) \exp(ik_z z),$$

where

$$\vec{B}_{n1}^{g\pm} = \frac{2(-i)^{n-1}}{a_1 \sqrt{\alpha^2 - |\vec{k}_{\parallel} + \vec{g}|^2}} \exp(in\phi_{k\alpha g}^s)(\vec{k}_{\alpha g}^{\pm} + k_z \hat{e}_z),$$

$$\vec{B}_{n2}^{g\pm} = \frac{2(-i)^{n-1}}{a_1 \sqrt{\beta^2 - |\vec{k}_{\parallel} + \vec{g}|^2}} \exp(in\phi_{k\beta g}^s)(\vec{k}_{\beta g}^{\pm} \times \hat{e}_z), \quad (30)$$

$$\vec{B}_{n3}^{g\pm} = \frac{2(-i)^{n-2}}{a_1 \sqrt{\beta^2 - |\vec{k}_{\parallel} + \vec{g}|^2}} \exp(in\phi_{k\beta g}^s)\left(\frac{k_z}{\beta} \vec{k}_{\beta g}^{\pm} - \beta \hat{e}_z\right),$$

and the sign + means $y > 0$ and $-$ means $y < 0$. Thus,

$$\vec{u}^{sc}(\vec{r}) = \vec{u}_{\alpha}^{sc\pm}(\vec{r}) + \vec{u}_{\beta}^{sc\pm}(\vec{r})$$

$$= \sum_{g} \vec{V}_{\alpha g}^{sc\pm} \exp(i\vec{k}_{\alpha g}^{\pm} \cdot \vec{\rho}) \exp(ik_z z) + \sum_{g} \vec{V}_{\beta g}^{sc\pm} \exp(i\vec{k}_{\beta g}^{\pm} \cdot \vec{\rho}) \exp(ik_z z), \quad (31)$$

where

$$\vec{V}_{\alpha g}^{sc\pm} = \sum_{n} b_{n1} \vec{B}_{n1}^{g\pm},$$

$$\vec{V}_{\beta g}^{sc\pm} = \sum_{n} (b_{n2} \vec{B}_{n2}^{g\pm} + b_{n3} \vec{B}_{n3}^{g\pm}). \quad (32)$$

By substituting equation (23) into (27) and then substituting the resulting expression into equation (32), we obtain

$$\vec{V}_{\alpha g}^{scs} = \sum_{s'g'} (M_{\alpha g \alpha g'}^{ss'} \cdot \vec{V}_{\alpha g'}^{ins'} + M_{\alpha g \beta g'}^{ss'} \cdot \vec{V}_{\beta g'}^{ins'}),$$

$$\vec{V}_{\beta g}^{scs} = \sum_{s'g'} (M_{\beta g \alpha g'}^{ss'} \cdot \vec{V}_{\alpha g'}^{ins'} + M_{\beta g \beta g'}^{ss'} \cdot \vec{V}_{\beta g'}^{ins'}), \quad (33)$$

where $M_{kk'}^{ss'}$ is defined as

$$M_{\alpha g \alpha g'}^{ss'} = \sum_{nn'} \vec{B}_{n1}^{gs} Z_{n1n'1} \vec{A}_{n'1}^{g's'},$$

$$M_{\alpha g \beta g'}^{ss'} = \sum_{nn'} (\vec{B}_{n1}^{gs} Z_{n1n'2} \vec{A}_{n'2}^{g's'} + \vec{B}_{n1}^{gs} Z_{n1n'3} \vec{A}_{n'3}^{g's'}),$$

$$M_{\beta g \alpha g'}^{ss'} = \sum_{nn'} (\vec{B}_{n2}^{gs} Z_{n2n'1} \vec{A}_{n'1}^{g's'} + \vec{B}_{n3}^{gs} Z_{n3n'1} \vec{A}_{n'1}^{g's'}), \quad (34)$$

$$M_{\beta g \beta g'}^{ss'} = \sum_{nn'} (\vec{B}_{n2}^{gs} Z_{n2n'2} \vec{A}_{n'2}^{g's'} + \vec{B}_{n2}^{gs} Z_{n2n'3} \vec{A}_{n'3}^{g's'} + \vec{B}_{n3}^{gs} Z_{n3n'2} \vec{A}_{n'2}^{g's'} + \vec{B}_{n3}^{gs} Z_{n3n'3} \vec{A}_{n'3}^{g's'}).$$

Equation (33) may be expressed in matrix form:

$$
\begin{bmatrix} \vec{V}_\alpha^{sc+} \\ \vec{V}_\beta^{sc+} \end{bmatrix} = \begin{bmatrix} M_{\alpha\alpha}^{++} & M_{\alpha\beta}^{++} \\ M_{\beta\alpha}^{++} & M_{\beta\beta}^{++} \end{bmatrix} \cdot \begin{bmatrix} \vec{V}_\alpha^{in+} \\ \vec{V}_\beta^{in+} \end{bmatrix} + \begin{bmatrix} M_{\alpha\alpha}^{+-} & M_{\alpha\beta}^{+-} \\ M_{\beta\alpha}^{+-} & M_{\beta\beta}^{+-} \end{bmatrix} \cdot \begin{bmatrix} \vec{V}_\alpha^{in-} \\ \vec{V}_\beta^{in-} \end{bmatrix},
$$
$$
\begin{bmatrix} \vec{V}_\alpha^{sc-} \\ \vec{V}_\beta^{sc-} \end{bmatrix} = \begin{bmatrix} M_{\alpha\alpha}^{-+} & M_{\alpha\beta}^{-+} \\ M_{\beta\alpha}^{-+} & M_{\beta\beta}^{-+} \end{bmatrix} \cdot \begin{bmatrix} \vec{V}_\alpha^{in+} \\ \vec{V}_\beta^{in+} \end{bmatrix} + \begin{bmatrix} M_{\alpha\alpha}^{--} & M_{\alpha\beta}^{--} \\ M_{\beta\alpha}^{--} & M_{\beta\beta}^{--} \end{bmatrix} \cdot \begin{bmatrix} \vec{V}_\alpha^{in-} \\ \vec{V}_\beta^{in-} \end{bmatrix},
$$

(35)

where $\vec{V}_k^{ins}$ and $\vec{V}_k^{scs}$ are column matrices and $M_{kk'}^{ss'}$ are square matrices, defined as

$$
\vec{V}_k^{ins} = [\ \vec{V}_{kg_1}^{ins} \quad \vec{V}_{kg_2}^{ins} \quad \cdots \quad \vec{V}_{kg_{n-1}}^{ins} \quad \vec{V}_{kg_n}^{ins}\ ]^{Tr},
$$
$$
\vec{V}_k^{scs} = [\ \vec{V}_{kg_1}^{scs} \quad \vec{V}_{kg_2}^{scs} \quad \cdots \quad \vec{V}_{kg_{n-1}}^{scs} \quad \vec{V}_{kg_n}^{scs}\ ]^{Tr},
$$

(36)

$$
M_{kk'}^{ss'} = \begin{bmatrix} M_{kg_1k'g_1}^{ss'} & M_{kg_1k'g_2}^{ss'} & \cdots & M_{kg_1k'g_{n-1}}^{ss'} & M_{kg_1k'g_n}^{ss'} \\ M_{kg_2k'g_1}^{ss'} & M_{kg_2k'g_2}^{ss'} & \cdots & M_{kg_2k'g_{n-1}}^{ss'} & M_{kg_2k'g_n}^{ss'} \\ \vdots & \vdots & \ddots & \vdots & \vdots \\ M_{kg_{n-1}k'g_1}^{ss'} & M_{kg_{n-1}k'g_2}^{ss'} & \cdots & M_{kg_{n-1}k'g_{n-1}}^{ss'} & M_{kg_{n-1}k'g_n}^{ss'} \\ M_{kg_nk'g_1}^{ss'} & M_{kg_nk'g_2}^{ss'} & \cdots & M_{kg_nk'g_{n-1}}^{ss'} & M_{kg_nk'g_n}^{ss'} \end{bmatrix}.
$$

(37)

The $M_{kk'}^{ss'}$ give the scattering of the incident plane elastic waves by a layer of periodically arranged scatterers.

4. Calculation of the transmission and reflection coefficients

To facilitate the derivation of the relevant formulae that follow, we write the displacement fields on both sides of the scattering plane in an alternative way. By naming the left side side 1 and the right side side 2, the wave travelling from the left to the right on side 1 and that along the opposite direction may be written as

$$
\begin{bmatrix} \vec{V}_\alpha^+(1) \\ \vec{V}_\beta^+(1) \end{bmatrix} = \begin{bmatrix} \vec{V}_\alpha^{in+} \\ \vec{V}_\beta^{in+} \end{bmatrix},
$$
$$
\begin{bmatrix} \vec{V}_\alpha^-(1) \\ \vec{V}_\beta^-(1) \end{bmatrix} = \begin{bmatrix} \vec{V}_\alpha^{sc-} \\ \vec{V}_\beta^{sc-} \end{bmatrix} + \begin{bmatrix} \vec{V}_\alpha^{in-} \\ \vec{V}_\beta^{in-} \end{bmatrix}.
$$

(38)

Similarly, on the right side, i.e., side 2, we have

$$
\begin{bmatrix} \vec{V}_\alpha^+(2) \\ \vec{V}_\beta^+(2) \end{bmatrix} = \begin{bmatrix} \vec{V}_\alpha^{in+} \\ \vec{V}_\beta^{in+} \end{bmatrix} + \begin{bmatrix} \vec{V}_\alpha^{sc+} \\ \vec{V}_\beta^{sc+} \end{bmatrix},
$$
$$
\begin{bmatrix} \vec{V}_\alpha^-(2) \\ \vec{V}_\beta^-(2) \end{bmatrix} = \begin{bmatrix} \vec{V}_\alpha^{in-} \\ \vec{V}_\beta^{in-} \end{bmatrix}.
$$

(39)

Substituting equation (35) into (38) and (39), we obtain

$$
\begin{bmatrix} \vec{V}_\alpha^+(2) \\ \vec{V}_\beta^+(2) \end{bmatrix} = \begin{bmatrix} I + M_{\alpha\alpha}^{++} & M_{\alpha\beta}^{++} \\ M_{\beta\alpha}^{++} & I + M_{\beta\beta}^{++} \end{bmatrix} \cdot \begin{bmatrix} \vec{V}_\alpha^+(1) \\ \vec{V}_\beta^+(1) \end{bmatrix} + \begin{bmatrix} M_{\alpha\alpha}^{+-} & M_{\alpha\beta}^{+-} \\ M_{\beta\alpha}^{+-} & M_{\beta\beta}^{+-} \end{bmatrix} \cdot \begin{bmatrix} \vec{V}_\alpha^-(2) \\ \vec{V}_\beta^-(2) \end{bmatrix},
$$
$$
\begin{bmatrix} \vec{V}_\alpha^-(1) \\ \vec{V}_\beta^-(1) \end{bmatrix} = \begin{bmatrix} M_{\alpha\alpha}^{-+} & M_{\alpha\beta}^{-+} \\ M_{\beta\alpha}^{-+} & M_{\beta\beta}^{-+} \end{bmatrix} \cdot \begin{bmatrix} \vec{V}_\alpha^+(1) \\ \vec{V}_\beta^+(1) \end{bmatrix} + \begin{bmatrix} I + M_{\alpha\alpha}^{--} & M_{\alpha\beta}^{--} \\ M_{\beta\alpha}^{--} & I + M_{\beta\beta}^{--} \end{bmatrix} \cdot \begin{bmatrix} \vec{V}_\alpha^-(2) \\ \vec{V}_\beta^-(2) \end{bmatrix}.
$$

(40)

One should note that all the plane-wave expansions, including the incident and scattered waves, are referred to the central scatterer in the plane. If we shift the centre of expansion by $-\vec{a}_2/2$

for waves on side 1 and by $\vec{a}_2/2$ for waves on side 2, where $\vec{a}_2$ is the translation vector of the 1D layer in forming a 2D crystal (as shown in figure 1), then

$$
\begin{bmatrix} \vec{V}_\alpha^+(2) \\ \vec{V}_\beta^+(2) \end{bmatrix} = \begin{bmatrix} Q_{\alpha\alpha}^{++} & Q_{\alpha\beta}^{++} \\ Q_{\beta\alpha}^{++} & Q_{\beta\beta}^{++} \end{bmatrix} \cdot \begin{bmatrix} \vec{V}_\alpha^+(1) \\ \vec{V}_\beta^+(1) \end{bmatrix} + \begin{bmatrix} Q_{\alpha\alpha}^{+-} & Q_{\alpha\beta}^{+-} \\ Q_{\beta\alpha}^{+-} & Q_{\beta\beta}^{+-} \end{bmatrix} \cdot \begin{bmatrix} \vec{V}_\alpha^-(2) \\ \vec{V}_\beta^-(2) \end{bmatrix},
$$

$$
\begin{bmatrix} \vec{V}_\alpha^-(1) \\ \vec{V}_\beta^-(1) \end{bmatrix} = \begin{bmatrix} Q_{\alpha\alpha}^{-+} & Q_{\alpha\beta}^{-+} \\ Q_{\beta\alpha}^{-+} & Q_{\beta\beta}^{-+} \end{bmatrix} \cdot \begin{bmatrix} \vec{V}_\alpha^+(1) \\ \vec{V}_\beta^+(1) \end{bmatrix} + \begin{bmatrix} Q_{\alpha\alpha}^{--} & Q_{\alpha\beta}^{--} \\ Q_{\beta\alpha}^{--} & Q_{\beta\beta}^{--} \end{bmatrix} \cdot \begin{bmatrix} \vec{V}_\alpha^-(2) \\ \vec{V}_\beta^-(2) \end{bmatrix}.
$$

(41)

where

$$
\vec{Q}_{kk'}^{ss'} = \phi_k^s \phi_{k'}^{s'} \delta_{kk'} \delta_{ss'} + \phi_k^s M_{kk'}^{ss'} \phi_{k'}^{s'},
$$

(42)

with matrices ϕ_k^s defined as

$$
\phi_k^s = \begin{bmatrix} \exp(si\vec{k}_{kg_1}^s \cdot \vec{a}_2/2) & & \\ & \ddots & \\ & & \exp(si\vec{k}_{kg_n}^s \cdot \vec{a}_2/2) \end{bmatrix}.
$$

(43)

Once the Q matrices for one scattering plane are determined, one can easily obtain the Q matrices of a slab with two scattering planes [15]. The procedure can be repeated to obtain the Q matrices for a slab with 2^n scattering planes, with n being an arbitrary integer. The proper combination of these slabs enables us to obtain the Q matrices for a slab with any number of scattering planes.

Once the Q matrices of a multilayer slab are obtained, we can completely determine the transmitted and reflected waves from equation (41), given incident waves. Since the flux is given by $(\lambda+2\mu)\omega(\vec{V}_{\alpha g}\cdot\vec{V}_{\alpha g}^*)\vec{k}_{\alpha g}$ and $\mu\omega(\vec{V}_{\beta g}\cdot\vec{V}_{\beta g}^*)\vec{k}_{\beta g}$ for a longitudinal plane elastic wave and transverse plane elastic wave, respectively, the transmittance T and reflectance R for elastic waves from a slab (with the normal direction along the y axis) is given by

$$
T(R) = \frac{\sum_g \{(\lambda + 2\mu)\vec{V}_{\alpha g}^{\text{trn(ref)}} \cdot \vec{V}_{\alpha g}^{\text{trn(ref)}*} k_{\alpha gy}^+ + \mu \vec{V}_{\beta g}^{\text{trn(ref)}} \cdot \vec{V}_{\beta g}^{\text{trn(ref)}*} k_{\beta gy}^+\}}{\sum_g \{(\lambda + 2\mu)\vec{V}_{\alpha g}^{\text{in}} \cdot \vec{V}_{\alpha g}^{\text{in}*} k_{\alpha gy}^+ + \mu \vec{V}_{\beta g}^{\text{in}} \cdot \vec{V}_{\beta g}^{\text{in}*} k_{\beta gy}^+\}} \quad (44)
$$

with $\vec{V}_{\alpha(\beta)g}^{\text{in}}$, $\vec{V}_{\alpha(\beta)g}^{\text{ref}}$ and $\vec{V}_{\alpha(\beta)g}^{\text{trn}}$ being components of the incident wave, reflected wave and transmitted wave, respectively, and $*$ denoting complex conjugation. The requirement for energy conservation implies that the absorbance ξ for a system with loss is given by

$$
\xi = 1 - T - R. \tag{45}
$$

5. Numerical results and discussion

To check our formalism and program, we first take a test band structure calculation for a 2D phononic crystal formed with Pb cylinders arranged in a square lattice in epoxy matrix with filling ratio $x = 0.30$, for which it had been shown in previous literature [8] that there exists a wide complete gap in the case of normal incidence, i.e., when the wavevector of incident wave has no component along the z direction. The materials parameters used in our calculation are $D = 11.4$ g cm^{-3}, $c_l = 2.16$ km s^{-1}, $c_l/c_t = 2.51$ for Pb, and $D = 1.18$ g cm^{-3}, $c_l = 2.54$ km s^{-1}, $c_l/c_t = 2.19$ for epoxy. Figure 2(a) shows the band structure calculated for the system when $k_z = 0$, which is in agreement with that calculated with 'pure' 2D MST [8]. This shows that our formalism and program are convincing. Moreover, the calculation is reasonable fast. For the case of 30% filling ratio, only about 20 min on an AMD Athlon 1.54 GHz machine (with 256 megabyte memory) is required to complete the whole band structure calculation.
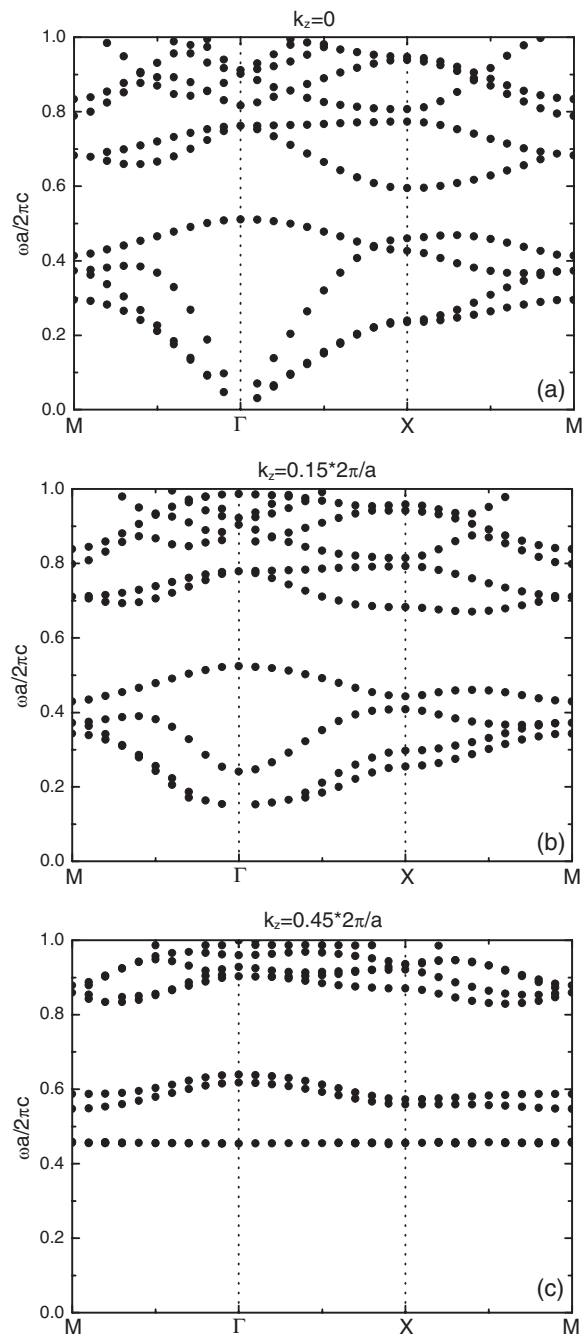
Figure 2. Band structures of elastic waves propagating in a square lattice consisting of Pb cylinders in epoxy matrix with filling ratio $x = 0.30$ for (a) $\gamma_z = 0$, (b) $\gamma_z = 0.15$, and (c) $\gamma_z = 0.45$. a is the lattice constant; c is the transverse velocity in epoxy.

Then we alter the normalized wavevector component $\gamma_z = k_z a/2\pi$ and increase it from zero gradually. Figures 2(b) and (c) show the band structures calculated when the normalized
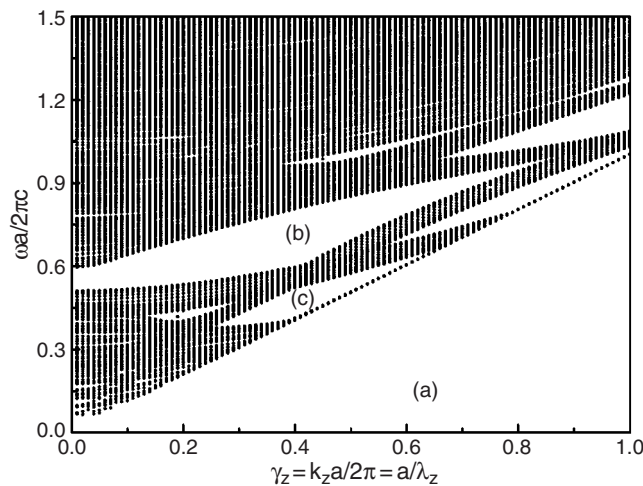
Figure 3. Projection of the phononic crystal band structure in the (k_x, k_y) plane onto the (k_z, ω) plane, for the phononic crystal consisting of Pb cylinders arranged in a square lattice in epoxy matrix with filling ratio $x = 0.30$. White regions indicate the absolute bandgaps in the (k_x, k_y) plane. a is the lattice constant; c is the transverse velocity in epoxy.

wavevector component γ_z equals 0.15 and 0.45, respectively. Evidently, the results for $\gamma_z = 0.15$ differ significantly from those for $\gamma_z = 0$. The most striking difference is that the dispersion curves for the lowest-frequency branches, in the case $\gamma_z \neq 0$, do not tend to zero anymore as both k_x and k_y tend to zero. As a result, a bandgap below the first band opens up in the phononic band structure for nonzero γ_z, whose width increases as γ_z increases [11].

In order to demonstrate the evolution of the elastic gaps more clearly, in figure 3 we show the projected band structures in the (k_x, k_y) plane onto the reduced frequency $\frac{\omega a}{2\pi c}$, normalized wavevector γ_z plane, where c is the transverse velocity in epoxy. The white regions indicate absolute bandgaps in the (k_x, k_y) plane. Several absolute bandgaps for nonzero out-of-plane wavevectors are visible, and no propagation and no vibration are allowed in these regions. The width of the low-frequency bandgap, labelled (a) in figure 3, increases monotonically from zero with increasing γ_z. When γ_z increases, the width of gap (b) that exist from $\frac{\omega a}{2\pi c} = 0.51$ to $\frac{\omega a}{2\pi c} = 0.60$ initially increases until $\gamma_z = 0.42$, then decreases and vanishes at $\gamma_z = 0.86$. Gap (c) appears at $\gamma_z = 0.26$ and vanishes at $\gamma_z = 0.64$. Evidently, there still exists a wide complete gap even if k_z is nonzero. It establishes that a high-density material arranged periodically in a low-density and relatively soft material always favours bandgaps, whether the incoming wave is normally or obliquely incident onto the 2D phononic crystal.

It is also evident in figure 3 that when the wavelength λ_z along the z axis is smaller than $a/0.4$ one isolated branch appears which is delimited by gap (a) and gap (c). If λ_z is kept constant, these modes are flat branches in the (k_x, k_y) plane, just like the lowest band already shown in figure 2(c). Consequently, their group velocities $(\partial\omega/\partial k_x, \partial\omega/\partial k_y)$ are zero in the (x, y) plane, and energy propagates along the cylinder axes [11, 12]. In addition, there are no allowed states from zero up to a certain frequency when k_z is greater than zero. This is because the slowest wave propagating in epoxy matrix is the bulk epoxy transverse mode, irrespective of the values of k_x and k_y. Then gap (a) always exists, and extends at least over the triangle below the bulk epoxy transverse mode, as shown in figure 3.

On the experimental side, usually the quantity which is the most convenient to measure is the transmission coefficient or the reflection coefficient of a finite phononic crystal slab. Thus
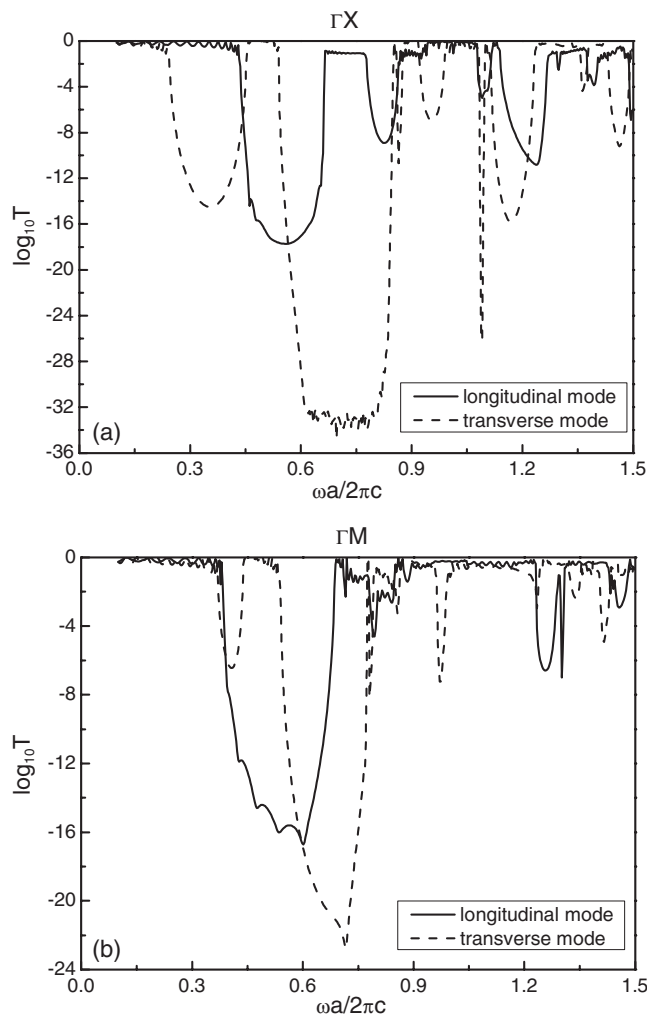
Figure 4. The transmission coefficients along the ΓX and ΓM directions of a 16-layer Pb–epoxy phononic crystal slab for a longitudinal incident wave (solid line) and for a transverse incident wave (dashed line for $\sigma = 2$ transverse mode) when the incident angle is $\theta = 25°$. a is the lattice constant; c is the transverse velocity in epoxy.

if we could figure out the transmittance or reflectance theoretically, it would make possible the straightforward comparison of the computational result with the experimental data. Based on this idea, in figure 4 we plot the transmission coefficient along the ΓX and ΓM directions of a 16-layer Pb–epoxy phononic crystal slab both for longitudinal incident wave and for transverse incident wave when the incident angle is $\theta = 25°$ (in this paper, the incident angle is defined as $\sin \theta = k_z/k$). Strictly speaking, the eigenmodes of the 2D phononic crystal are mixed modes, consisting of both longitudinal modes and transverse modes. However, if $\vec{k}_x = 0$, i.e., the incident wavevector has no component along the x direction, and the frequency is not very high, which is just the situation considered in this paper, only the $\vec{g} = 0$ component is a propagating wave and its amplitude is much larger than other components. Therefore, only the $\vec{g} = 0$ component will couple with the external incident wave. As a result, in the phononic crystal slab only longitudinal modes could be excited by a longitudinal incident wave and only
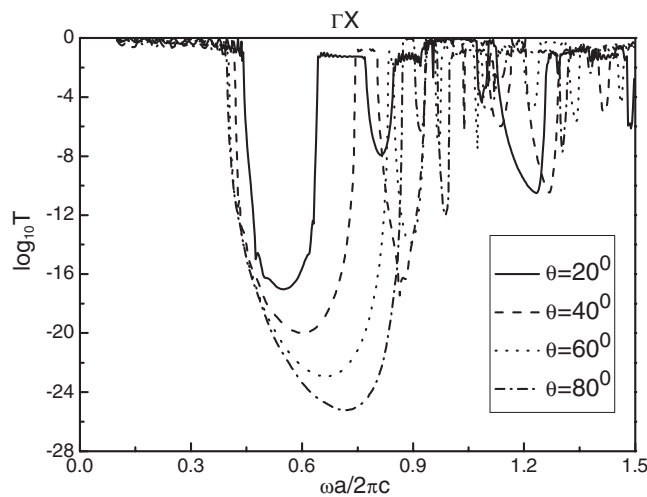
Figure 5. The transmission coefficients along the ΓX direction of a 16-layer Pb–epoxy phononic crystal slab for a longitudinal incident wave when the incident angle θ is 20°, 40°, 60° and 80°, respectively. a is the lattice constant; c is the transverse velocity in epoxy.

transverse modes could be excited by a transverse incident wave. But for higher frequency or for $\vec{k}_x \neq 0$, mixed modes could be easily excited. For this reason, we separate the transmission coefficient of the longitudinal mode from those of the transverse mode. As shown in figure 4, in the case of 25° incident angle, the first common bandgap for both the longitudinal mode and the transverse mode along the ΓM direction exist from $\frac{\omega a}{2\pi c} = 0.54$ to $\frac{\omega a}{2\pi c} = 0.67$, while along the ΓX direction the first common bandgap begins at $\frac{\omega a}{2\pi c} = 0.53$ and vanishes at $\frac{\omega a}{2\pi c} = 0.69$. Therefore, a complete bandgap exists in the range of (0.54–0.67) in the unit of the reduced frequency.

In fact, all the gaps will shift to the higher frequency range with increasing the incident angle θ whether the longitudinal mode or the transverse mode is concerned. For example, in figure 5 we plot the transmission coefficient along the ΓX direction of a 16-layer Pb–epoxy phononic crystal slab for a longitudinal incident wave when the incident angle θ is 20°, 40°, 60° and 80°, respectively. Evidently, as θ increases, the first gap becomes larger and larger and shifts to the higher frequency range, and at the same time all other the gaps also shift to the higher frequency range. It is easy to understand such a variation of gap with the incident angle. For a given frequency, the bigger the incident angle, the smaller the projection of the wavevector in the $x-y$ plane k_{xy}, which means that for a bigger incident angle we must increase the frequency in order to let the in-plane projection k_{xy} arrive at the threshold value at which the gap begins to exist for a smaller incident angle. As a result, the gap will shift to higher frequency for a bigger θ. It also gives us the suggestion that we could tailor the gap frequency range according to the demands by just tuning the incident angle of the incoming elastic wave without changing the structure of the 2D phononic crystal. In addition, the complete bandgap for different incident angles may have a common frequency range for a given structure. This property can be useful for technological applications of periodic structures such as the 'phononic crystal fibres', for which the propagation of elastic waves is along the normal to the periodic plane.

It is well known that the PW method cannot deal with the systems with mixed solid and fluid components, which include two cases: the first is the system formed with solid cylinders arranged in fluid, and the second is the reverse of the first, with fluid cylinders arranged in a solid matrix. In order to use the PW method to study the band structures of the system with
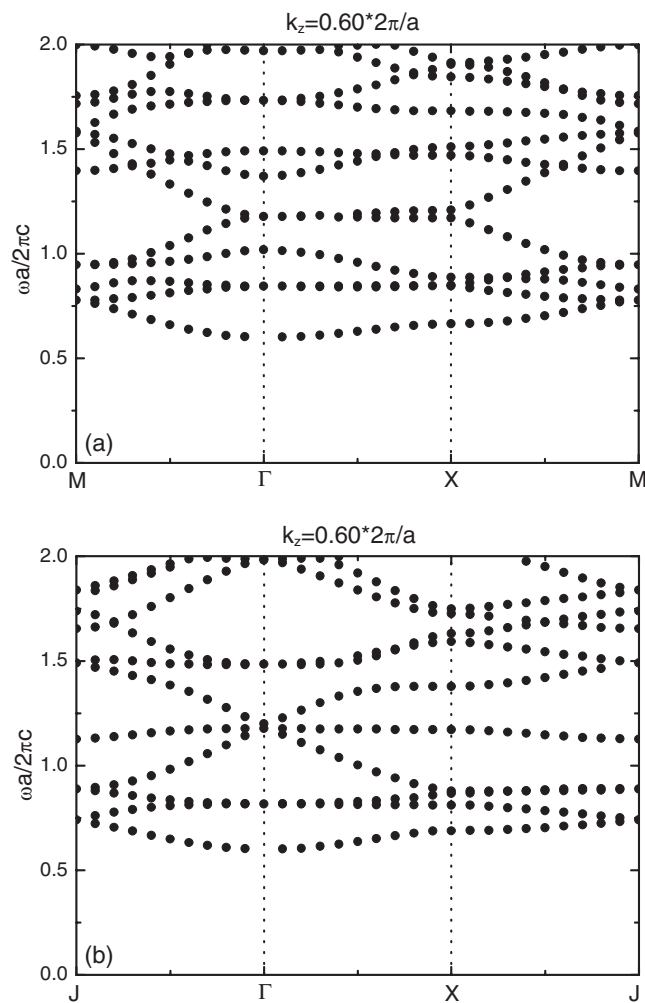
Figure 6. Band structures of acoustic wave in the phononic crystals consisting of Fe cylinders in water arranged in (a) a square lattice and (b) a hexagonal lattice, with filling ratio $x = 0.35$ for $\gamma_z = 0.60$. a is the lattice constant; c is the acoustic wave velocity in water.

solid inclusions in fluid, one has to neglect the transverse mode excited in solid inclusions and simply treat the solid as a fluid, where only longitudinal modes exist. This approximation only holds when the solid component is stiff enough that the wave propagation in the surrounding fluid can hardly refract into the solid. For the second case, the PW method completely fails. Recently, a treatment for the case is proposed by use of the PW method in which an artificial transverse velocity is introduced into the fluid [16]. However, the MST approach can easily handle the systems with mixed solid and fluid components, either a solid component in a fluid or a fluid component in a solid. In the following, we first apply our MST approach to calculate the band structure and transmission coefficient for Fe cylinders immersed in water, arranged in both a hexagonal lattice and a square lattice, and then calculate the band structure for the reverse problem, i.e., water-filled cylindrical holes drilled in a PMMA matrix.

Figures 6(a) and (b) show the band structures of acoustic waves for steel cylinders immersed in water arranged in a square lattice and a hexagonal lattice, respectively. Both
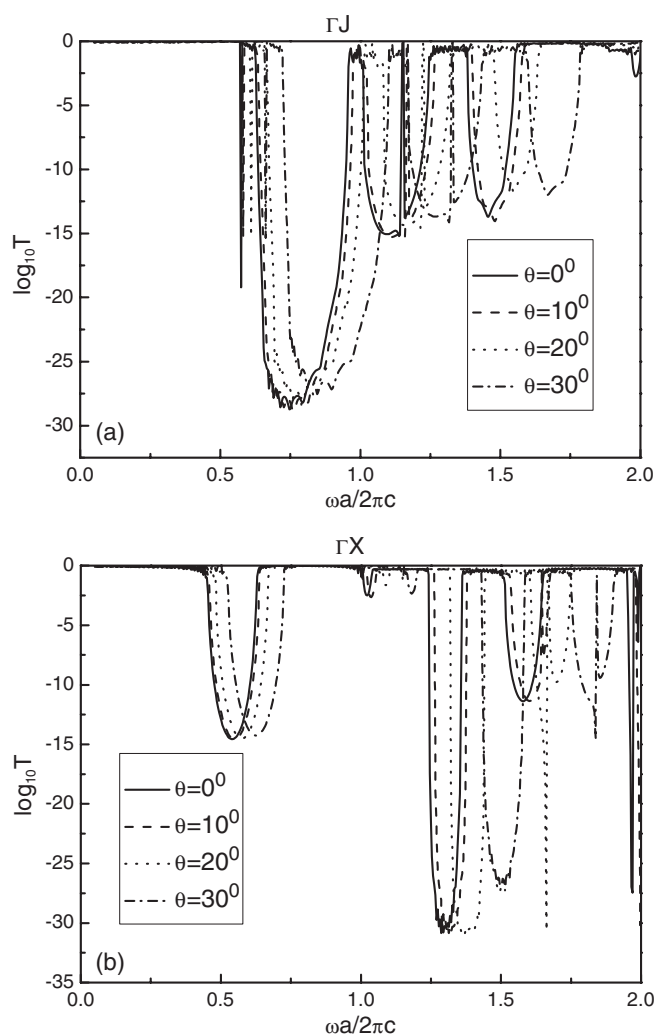
Figure 7. The transmission coefficients along the ΓJ and ΓX directions of a 32-layer Fe–water phononic crystal slab for a longitudinal incident wave when the incident angle θ is 0°, 10°, 20° and 30°, respectively. a is the lattice constant; c is the acoustic wave in water.

structures have the same filling ratio 0.35. The material parameters used here are $D = 1.0$ g cm^{-3}, $c_l = 1.49$ km s^{-1} for water, and $D = 7.67$ g cm^{-3}, $c_l = 6.01$ km s^{-1}, $c_l/c_t = 1.86$ for steel. As shown in figure 6, bandgaps are not observed in the case of $\gamma_z = 0.6$ when the filling fraction is 0.35. In fact, at this filling fraction, the complete bandgap is very small for a square lattice and does not exist for a hexagonal lattice even in the case of normal incidence, i.e., $\gamma_z = 0$. In order to create and enlarge the complete bandgap for a nonzero γ_z value, an effective method is to increasing the filling fraction of the Fe cylinders, which has already been verified by our band structure calculations not shown here.

Moreover, we could plot the transmission–frequency curve for the Fe–water system as we have done for the solid–solid system. Since only a longitudinal wave could propagate in the fluid matrix, we merely need to consider the longitudinal incident mode now. In figure 7, we plot the transmission coefficients along the two high symmetry directions for a hexagonal
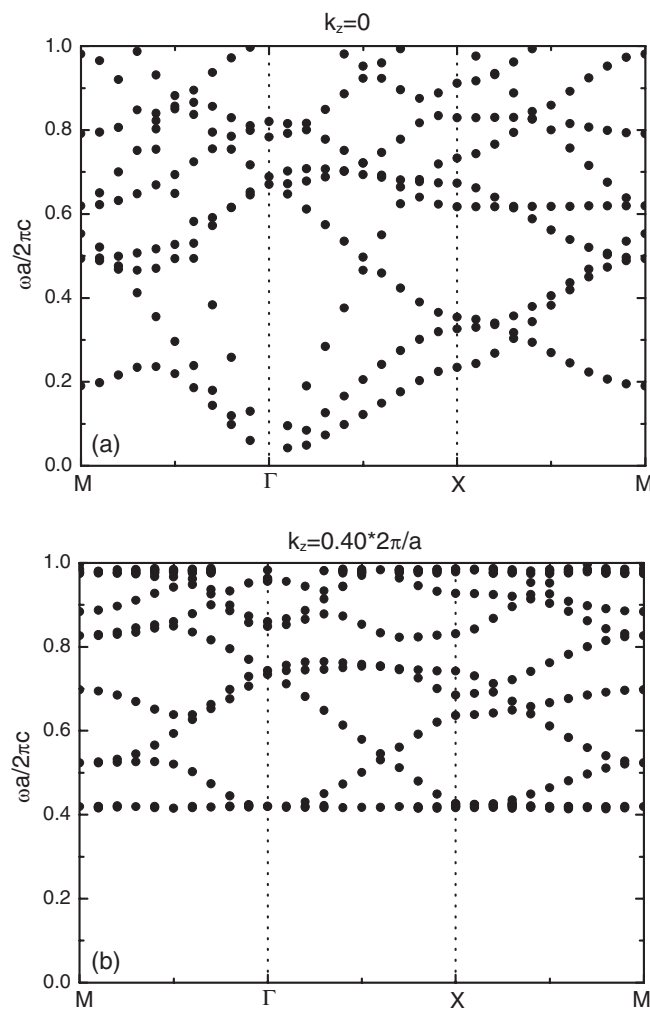
Figure 8. Band structures of elastic waves in the phononic crystals consisting of water cylinders in a PMMA matrix arranged in a square lattice, with filling ratio $x = 0.40$ for (a) $\gamma_z = 0$, and (b) $\gamma_z = 0.40$. a is the lattice constant; c is the transverse velocity in PMMA.

lattice, i.e., ΓJ and ΓX directions, of a 32-layer Fe–water phononic crystal slab when the incident angle θ is $0°$, $10°$, $20°$ and $30°$, respectively. The same as the solid–solid phononic crystal, all the gaps will shift to higher frequency range with the increase of θ for both the ΓJ and the ΓX directions. This behaviour can be explained with a similar analysis as above.

For the reverse problem, i.e., water cylinders in a PMMA matrix, it is a little complex; three kinds of modes coexist in such a case. Figure 8 shows the band structures for a phononic crystal consisting of water cylinders arranged in a square lattice in a PMMA matrix with filling fraction $x = 0.40$. As shown, there is no gap for both in-plane propagation and out-of-plane propagation with $\gamma_z = 0.4$. Further calculations indicate that there is no gap in the whole range of the filling fraction for any value of k_z component. For water cylinders arranged in a PMMA matrix in a hexagonal lattice no gap is found either. It seems that it is really a difficulty to realize the bandgap in such a system.

6. Concluding remarks

In summary, we have extended the multiple-scattering theory to out-of-plane propagating elastic waves in 2D composite and show that the approach has a rapid convergence speed in both the band structure and the transmission coefficient calculations for 2D phononic crystals composed of cylinders in a matrix material. An interesting advantage is its power in handling the system with mixing solid and fluid components for which the plane wave method complete fails. The application of the MST approach to three 2D systems, that is, lead cylinders in epoxy, steel cylinders in water, and water cylinders in a PMMA matrix, are calculated.

Acknowledgments

Appendix A

In this appendix, we prove equations (9) and (10), where the vector structure constant $G_{n\sigma n'\sigma'}$ is defined by the relation

$$\vec{H}_{n\sigma}(\vec{r} - \vec{R}) = \sum_{n'\sigma'} G_{n\sigma n'\sigma'}(\vec{R}) \vec{J}_{n'\sigma'}(\vec{r}). \tag{A.1}$$

It is known that

$$H_n(k|\vec{\rho} - \vec{\rho}'|) e^{in\phi''} = \begin{cases} \displaystyle\sum_{n'=-\infty}^{\infty} J_{n'-n}(k\rho') H_{n'}(k\rho) e^{in'\phi - i(n'-n)\phi'} & \rho > \rho' \\ \displaystyle\sum_{n'=-\infty}^{\infty} H_{n'-n}(k\rho') J_{n'}(k\rho) e^{in'\phi - i(n'-n)\phi'} & \rho < \rho', \end{cases} \tag{A.2}$$

where ϕ, ϕ' and ϕ'' are the arguments of $\vec{\rho}$, $\vec{\rho}'$ and $\vec{\rho} - \vec{\rho}'$, respectively. Because $\rho < R$ is always satisfied since the field point is within a unit cell, we have

$$H_n(\alpha|\vec{\rho} - \vec{R}|) e^{in\phi''} = \sum_{n'} H_{n'-n}(\alpha R) e^{-i(n'-n)\phi'} J_{n'}(\alpha\rho) e^{in'\phi}$$

$$= \sum_{n'} X_{nn'}^{\alpha}(\vec{R}) J_{n'}(\alpha\rho) e^{in'\phi}, \tag{A.3}$$

where $X_{nn'}^{\alpha}(\vec{R}) = H_{n'-n}(\alpha R) e^{-i(n'-n)\phi'}$, and ϕ, ϕ', and ϕ'' are the arguments of $\vec{\rho}$, $\vec{R}$, and $\vec{\rho} - \vec{R}$, respectively.

Since the translation vector $\vec{R}$ is always in the x–y plane, by decomposing the vector $\vec{r} - \vec{R}$ as $\vec{r} - \vec{R} = (\vec{\rho} + z\hat{e}_z) - \vec{R} = (\vec{\rho} - \vec{R}) + z\hat{e}_z$, we have

$$\vec{H}_{n1}(\vec{r} - \vec{R}) = \vec{H}_{n1}((\vec{\rho} - \vec{R}) + z\hat{e}_z)$$

$$= \nabla[H_n(\alpha|\vec{\rho} - \vec{R}|) e^{in\phi''} e^{ik_z z}]$$

$$= \nabla\left[\sum_{n'} X_{nn'}^{\alpha}(\vec{R}) J_{n'}(\alpha\rho) e^{in'\phi} e^{ik_z z}\right]$$

$$= \sum_{n'} X_{nn'}^{\alpha}(\vec{R}) \nabla[J_{n'}(\alpha\rho) e^{in'\phi} e^{ik_z z}]$$

$$= \sum_{n'} X^{\alpha}_{nn'}(\vec{R}) \vec{J}_{n'1}(\vec{r})$$

$$= \sum_{n'\sigma'} X^{\alpha}_{nn'}(\vec{R}) \delta_{1\sigma'} \vec{J}_{n'\sigma'}(\vec{r}). \tag{A.4}$$

Comparison of equation (A.1) with the last line of equation (A.4) gives

$$G_{n1n'\sigma'}(\vec{R}) = X^{\alpha}_{nn'}(\vec{R}) \delta_{1\sigma'}. \tag{A.5}$$

We now turn to $\vec{H}_{n2}(\vec{r} - \vec{R})$; we see that

$$\begin{aligned}
\vec{H}_{n2}(\vec{r} - \vec{R}) &= \vec{H}_{n2}((\vec{\rho} - \vec{R}) + z\hat{e}_z) \\
&= \nabla \times [\hat{e}_z H_n(\beta|\vec{\rho} - \vec{R}|) \mathrm{e}^{\mathrm{i}n\phi''} \mathrm{e}^{\mathrm{i}k_z z}] \\
&= \nabla \times \left[\sum_{n'} X^{\beta}_{nn'}(\vec{R}) \hat{e}_z J_{n'}(\beta\rho) \mathrm{e}^{\mathrm{i}n'\phi} \mathrm{e}^{\mathrm{i}k_z z} \right] \\
&= \sum_{n'} X^{\beta}_{nn'}(\vec{R}) \nabla \times [\hat{e}_z J_{n'}(\beta\rho) \mathrm{e}^{\mathrm{i}n'\phi} \mathrm{e}^{\mathrm{i}k_z z}] \\
&= \sum_{n'} X^{\beta}_{nn'}(\vec{R}) \vec{J}_{n'2}(\vec{r}),
\end{aligned} \tag{A.6}$$

from which we obtain

$$G_{n2n'\sigma'}(\vec{R}) = X^{\beta}_{nn'}(\vec{R}) \delta_{2\sigma'}. \tag{A.7}$$

To get the expression for $\vec{H}_{n3}(\vec{r} - \vec{R})$, we use $(1/\beta)\nabla \times$ to act on equation (A.6), leading to

$$\begin{aligned}
\vec{H}_{n3}(\vec{r} - \vec{R}) &= \frac{1}{\beta} \nabla \times \left[\sum_{n'} X^{\beta}_{nn'}(\vec{R}) \vec{J}_{n'2}(\vec{r}) \right] \\
&= \sum_{n'} X^{\beta}_{nn'}(\vec{R}) \left[\frac{1}{\beta} \nabla \times \vec{J}_{n'2}(\vec{r}) \right] \\
&= \sum_{n'} X^{\beta}_{nn'}(\vec{R}) \vec{J}_{n'3}(\vec{r}),
\end{aligned} \tag{A.8}$$

from which we get

$$G_{n3n'\sigma'}(\vec{R}) = X^{\beta}_{nn'}(\vec{R}) \delta_{3\sigma'}. \tag{A.9}$$

Appendix B

In this appendix, we prove equations (23) and (24). According to equation (18), we have

$$\vec{V}^{\mathrm{in}\pm}_{\alpha g}(\vec{r}) \parallel (\vec{k}^{\pm}_{\alpha g} + k_z \hat{e}_z). \tag{B.1}$$

By using the identity

$$\exp(\mathrm{i}\vec{k}^s_{\alpha g} \cdot \vec{\rho}) = \sum_n \mathrm{i}^n J_n(\alpha\rho) \exp[-\mathrm{i}n(\phi^s_{\vec{k}\alpha g} - \phi_{\vec{\rho}})], \tag{B.2}$$

with $\phi^s_{\vec{k}\alpha g}$ denoting the azimuth angle of $\vec{k}^s_{\alpha g}$, we can obtain that

$$\begin{aligned}
\vec{V}^{\mathrm{ins}}_{\alpha g} & \exp(\mathrm{i}\vec{k}^s_{\alpha g} \cdot \vec{\rho}) \exp(\mathrm{i}k_z z) \\
&= \vec{V}^{\mathrm{ins}}_{\alpha g} \cdot \frac{\vec{k}^s_{\alpha g} + k_z \hat{e}_z}{\mathrm{i}|\vec{k}^s_{\alpha g} + k_z \hat{e}_z|^2} \nabla \exp[\mathrm{i}(\vec{k}^s_{\alpha g} + k_z \hat{e}_z) \cdot (\vec{\rho} + z\hat{e}_z)]
\end{aligned}$$

$$= \vec{V}_{\alpha g}^{\mathrm{ins}} \cdot \frac{\vec{k}_{\alpha g}^s + k_z \hat{e}_z}{\mathrm{i}(\alpha^2 + k_z^2)} \nabla \left\{ \sum_n \mathrm{i}^n J_n(\alpha \rho) \exp[-\mathrm{i}n(\phi_{\vec{k}\alpha g}^s - \phi_{\vec{\rho}})] \exp(\mathrm{i}k_z z) \right\}$$

$$= \sum_n \frac{\mathrm{i}^{n-1}}{\alpha^2 + k_z^2} \vec{V}_{\alpha g}^{\mathrm{ins}} \cdot (\vec{k}_{\alpha g}^s + k_z \hat{e}_z) \exp(-\mathrm{i}n\phi_{\vec{k}\alpha g}^s) \vec{J}_{n1}(\vec{r}). \tag{B.3}$$

Since

$$\vec{u}_\alpha^{\mathrm{in}}(\vec{r}) = \sum_{sg} \vec{V}_{\alpha g}^{\mathrm{ins}} \exp(\mathrm{i}\vec{k}_{\alpha g}^s \cdot \vec{\rho}) \exp(\mathrm{i}k_z z) = \sum_n a_{n1} \vec{J}_{n1}(\vec{r}), \tag{B.4}$$

we have

$$a_{n1} = \frac{\mathrm{i}^{n-1}}{\alpha^2 + k_z^2} \sum_{sg} \vec{V}_{\alpha g}^{\mathrm{ins}} \cdot (\vec{k}_{\alpha g}^s + k_z \hat{e}_z) \exp(-\mathrm{i}n\phi_{\vec{k}\alpha g}^s) = \sum_{sg} \vec{V}_{\alpha g}^{\mathrm{ins}} \cdot \vec{A}_{n1}^{gs}, \tag{B.5}$$

with

$$\vec{A}_{n1}^{gs} = \frac{\mathrm{i}^{n-1}}{\alpha^2 + k_z^2} \exp(-\mathrm{i}n\phi_{\vec{k}\alpha g}^s)(\vec{k}_{\alpha g}^s + k_z \hat{e}_z). \tag{B.6}$$

On the other hand, according to equation (18) we have

$$\vec{V}_{\beta g}^{\mathrm{ins}}(\vec{r}) \perp (\vec{k}_{\beta g}^s + k_z \hat{e}_z). \tag{B.7}$$

Moreover, if we define vector $\vec{m}_1$ and $\vec{m}_2$ as

$$\vec{m}_1 = \vec{k}_{\beta g}^s \times \hat{e}_z,$$
$$\vec{m}_2 = -\frac{k_z}{\beta} \vec{k}_{\beta g}^s + \beta \hat{e}_z, \tag{B.8}$$

we can prove that $\vec{m}_1 \perp \vec{m}_2 \perp (\vec{k}_{\beta g}^s + k_z \hat{e}_z)$. Then $\vec{V}_{\beta g}^{\mathrm{ins}}$ can be decomposed as the linear combination of $\vec{m}_1$ and $\vec{m}_2$:

$$\vec{V}_{\beta g}^{\mathrm{ins}}(\vec{r}) = l_1 \vec{m}_1 + l_2 \vec{m}_2, \tag{B.9}$$

with

$$l_1 = \vec{V}_{\beta g}^{\mathrm{ins}} \cdot (\vec{k}_{\beta g}^s \times k_z \hat{e}_z)/\beta^2,$$
$$l_2 = \vec{V}_{\beta g}^{\mathrm{ins}} \cdot \left(-\frac{k_z}{\beta} \vec{k}_{\beta g}^s + \beta \hat{e}_z \right) \bigg/ (\beta^2 + k_z^2) \tag{B.10}$$

so that

$$\vec{u}_\beta^{\mathrm{in}}(\vec{r}) = \sum_{sg} \vec{V}_{\beta g}^{\mathrm{ins}} \exp(\mathrm{i}\vec{k}_{\beta g}^s \cdot \vec{\rho}) \exp(\mathrm{i}k_z z)$$

$$= \sum_{sg} l_1 \vec{m}_1 \exp(\mathrm{i}\vec{k}_{\beta g}^s \cdot \vec{\rho}) \exp(\mathrm{i}k_z z) + \sum_{sg} l_2 \vec{m}_2 \exp(\mathrm{i}\vec{k}_{\beta g}^s \cdot \vec{\rho}) \exp(\mathrm{i}k_z z)$$

$$= \sum_{sg} \frac{l_1}{\mathrm{i}} \nabla \times [\hat{e}_z \exp(\mathrm{i}\vec{k}_{\beta g}^s \cdot \vec{\rho}) \exp(\mathrm{i}k_z z)]$$

$$+ \sum_{sg} \frac{l_2}{\beta} \nabla \times \nabla \times [\hat{e}_z \exp(\mathrm{i}\vec{k}_{\beta g}^s \cdot \vec{\rho}) \exp(\mathrm{i}k_z z)]$$

$$= \sum_{sg} \frac{l_1}{\mathrm{i}} \sum_n \mathrm{i}^n \exp(-\mathrm{i}n\phi_{\vec{k}\beta g}^s) \vec{J}_{n2}(\vec{r}) + \sum_{sg} \frac{l_2}{\beta} \sum_n \mathrm{i}^n \exp(-\mathrm{i}n\phi_{\vec{k}\beta g}^s) \vec{J}_{n3}(\vec{r})$$

$$= \sum_{sg} \sum_n \vec{V}_{\beta g}^{\mathrm{ins}} \cdot \frac{(\vec{k}_{\beta g}^s \times k_z \hat{e}_z)}{\beta^2} \mathrm{i}^{n-1} \exp(-\mathrm{i}n\phi_{\vec{k}\beta g}^s) \vec{J}_{n2}(\vec{r})$$

$$+ \sum_{sg} \sum_{n} \vec{V}_{\beta g}^{\text{ins}} \cdot \frac{-\frac{k_z}{\beta} \vec{k}_{\beta g}^{s} + \beta \hat{e}_z}{(\beta^2 + k_z^2)} \text{i}^n \exp(-\text{i}n\phi_{\vec{k}\beta g}^{s}) \vec{J}_{n3}(\vec{r})$$

$$= \sum_{n} \sum_{sg} \vec{V}_{\beta g}^{\text{ins}} \cdot \vec{A}_{n2}^{gs} \vec{J}_{n2}(\vec{r}) + \sum_{n} \sum_{sg} \vec{V}_{\beta g}^{\text{ins}} \cdot \vec{A}_{n3}^{gs} \vec{J}_{n3}(\vec{r})$$

$$= \sum_{n} [a_{n2} \vec{J}_{n2}(\vec{r}) + a_{n3} \vec{J}_{n3}(\vec{r})] \tag{B.11}$$

where

$$a_{n2} = \sum_{sg} \vec{V}_{\beta g}^{\text{ins}} \cdot A_{n2}^{gs},$$

$$\vec{A}_{n2}^{gs} = \frac{\text{i}^{n-1}}{\beta^2} \exp(-\text{i}n\phi_{\vec{k}\beta g}^{s})(\vec{k}_{\beta g}^{s} \times \hat{e}_z), \tag{B.12}$$

$$a_{n3} = \sum_{sg} \vec{V}_{\beta g}^{\text{ins}} \cdot A_{n3}^{gs},$$

$$\vec{A}_{n3}^{gs} = \frac{\text{i}^n}{\beta^2 + k_z^2} \exp(-\text{i}n\phi_{\vec{k}\beta g}^{s}) \left(-\frac{k_z}{\beta} \vec{k}_{\beta g}^{s} + \beta \hat{e}_z \right). \tag{B.13}$$

Appendix C

In addition to the externally incident wave, the incident wave for the central scatterer includes the contributions from all the other scatterers in the scattering plane:

$$\sum_{i \neq 0} \sum_{n\sigma} b_{n\sigma}^{i} \vec{H}_{n\sigma}(\vec{r}_i)$$

$$= \sum_{n\sigma} b_{n\sigma} {\sum_{\vec{R}}}' \exp(\text{i}\vec{k}_{\parallel} \cdot \vec{R}) \vec{H}_{n\sigma}(\vec{r} - \vec{R})$$

$$= \sum_{n\sigma} b_{n\sigma} {\sum_{\vec{R}}}' \exp(\text{i}\vec{k}_{\parallel} \cdot \vec{R}) \sum_{n'\sigma'} G_{n\sigma n'\sigma'}(-\vec{R}) \vec{J}_{n'\sigma'}(\vec{r})$$

$$= \sum_{n\sigma} a_{n\sigma}' \vec{J}_{n\sigma}(\vec{r}), \tag{C.1}$$

where

$$a_{n\sigma}' = \sum_{n'\sigma'} b_{n'\sigma'} G_{n'\sigma' n\sigma}(\vec{k}_{\parallel}). \tag{C.2}$$

For the explicit expression of $G_{n\sigma n'\sigma'}(\vec{k}_{\parallel})$, see equation (28). The total incident wave for the central scatterer in the plane is thus $\sum_{n\sigma} (a_{n\sigma} + a_{n\sigma}') \vec{J}_{n\sigma}(\vec{r})$. It follows that

$$b_{n\sigma} = \sum_{n'\sigma'} t_{n\sigma n'\sigma'} (a_{n'\sigma'} + a_{n'\sigma'}'), \tag{C.3}$$

where $T = \{t_{n\sigma n'\sigma'}\}$ is the scattering matrix of the central scatterer. To write equation (C.3) in the matrix form, we have

$$B = T(A + A') = T[A + G^{\text{Tr}}(\vec{k}_{\parallel})B]; \tag{C.4}$$

thus

$$B = ZA, \tag{C.5}$$

where the Z matrix is defined as

$$Z = [I - TG^{\text{Tr}}(\vec{k}_{\parallel})]^{-1} T, \tag{C.6}$$

with I being the unit matrix.

Appendix D

In this appendix, we prove equations (29) and (30). We first introduce the formula [17]

$$H_0(k\rho) = \frac{1}{\pi} \int_{-\infty}^{+\infty} \frac{\exp(ik'_x x + i\sqrt{k^2 - k'^2_x}|y|)}{\sqrt{k^2 - k'^2_x}} \, dk'_x = \frac{1}{\pi} \int_{-\infty}^{+\infty} \frac{\exp(i\vec{k}'^{\pm} \cdot \vec{\rho})}{\sqrt{k^2 - k'^2_x}} \, dk'_x \qquad (D.1)$$

where $\vec{k}'^{\pm} = (k'_x, \pm\sqrt{k^2 - k'^2_x})$, satisfying $|\vec{k}'^{\pm}| = k$, and the sign $+ (-)$ corresponds to $y > 0$ $(y < 0)$. If $k'^2_x > k^2$, $\sqrt{k^2 - k'^2_x}$ takes the value $i\sqrt{k'^2_x - k^2}$.

By using another identity

$$\exp(-i\vec{k}'^{\pm} \cdot \vec{\rho}_0) = \sum_{n=-\infty}^{+\infty} (-i)^n \exp(-in\phi^{\pm}_{\vec{k}'} + in\phi_{\vec{\rho}_0}) J_n(k\rho_0), \qquad (D.2)$$

with $\phi^{\pm}_{\vec{k}'}$ being the azimuth angle of $\vec{k}'^{\pm}$, we can get

$$H_0(k|\vec{\rho} - \vec{\rho}_0|) = \frac{1}{\pi} \int_{-\infty}^{+\infty} \frac{\exp(i\vec{k}'^{\pm} \cdot \vec{\rho})}{\sqrt{k^2 - k'^2_x}} \left[\sum_{n=-\infty}^{+\infty} (-i)^n \exp(-in\phi^{\pm}_{\vec{k}'} + in\phi_{\vec{\rho}_0}) J_n(k\rho_0) \right] dk'_x.$$
$$(D.3)$$

In the cylindrical coordinates, if $\rho > \rho_0$, the addition theorem gives

$$H_0(k|\vec{\rho} - \vec{\rho}_0|) = \sum_{n=-\infty}^{+\infty} J_n(k\rho_0) H_n(k\rho) \exp[in(\phi_{\vec{\rho}} - \phi_{\vec{\rho}_0})]. \qquad (D.4)$$

Multiplying equations (D.3) and (D.4) by $\exp(im\phi_{\vec{\rho}_0})$ and integrating $\phi_{\vec{\rho}_0}$ from 0 to 2π and eliminating the item $J_m(k\rho_0)$, we can establish that

$$H_n(k\rho) \exp(in\phi_{\vec{\rho}}) = \frac{(-i)^n}{\pi} \int_{-\infty}^{+\infty} \frac{\exp(i\vec{k}'^{\pm} \cdot \vec{\rho})}{\sqrt{k^2 - k'^2_x}} \exp(in\phi^{\pm}_{\vec{k}'}) \, dk'_x. \qquad (D.5)$$

Therefore

$$\sum_{\vec{R}} H_n(k|\vec{\rho} - \vec{R}|) \exp(in\phi_{\vec{\rho}-\vec{R}}) \exp(ik_z z) \exp(i\vec{k}_{\parallel} \cdot \vec{R})$$

$$= \frac{(-i)^n}{\pi} \int_{-\infty}^{+\infty} \frac{\exp(i\vec{k}'^{\pm} \cdot \vec{\rho})}{\sqrt{k^2 - k'^2_x}} \exp(in\phi^{\pm}_{\vec{k}'}) \exp(ik_z z) \sum_{\vec{R}} \exp[i(\vec{k}_{\parallel} - \vec{k}'^{\pm}) \cdot \vec{R}] \, dk'_x.$$
$$(D.6)$$

Noting that

$$\sum_{\vec{R}} \exp[i(\vec{k}_{\parallel} - \vec{k}'^{\pm}) \cdot \vec{R}] = \frac{2\pi}{a_1} \sum_{g} \delta(\vec{k}_{\parallel} + \vec{g} - k'_x \hat{e}_x), \qquad (D.7)$$

we have

$$\sum_{\vec{R}} H_n(k|\vec{\rho} - \vec{R}|) \exp(in\phi_{\vec{\rho}-\vec{R}}) \exp(ik_z z) \exp(i\vec{k}_{\parallel} \cdot \vec{R})$$

$$= \frac{2(-i)^n}{a_1} \sum_{g} \frac{\exp(i\vec{k}^{\pm}_g \cdot \vec{\rho})}{\sqrt{k^2 - |\vec{k}_{\parallel} + \vec{g}|^2}} \exp(in\phi^{\pm}_{\vec{k}_g}) \exp(ik_z z), \qquad (D.8)$$

with

$$\vec{k}^{\pm}_g = \left(\vec{k}_{\parallel} + \vec{g}, \pm\sqrt{k^2 - |\vec{k}_{\parallel} + \vec{g}|^2} \right) \qquad (D.9)$$

and $\phi^{\pm}_{\vec{k}_g}$ being the argument of $\vec{k}^{\pm}_g$.

According to equation (D.8), we can establish that

$$\sum_{\vec{R}} \exp(i\vec{k}_\parallel \cdot \vec{R}) \vec{H}_{n1}(\vec{r} - \vec{R})$$

$$= \nabla \left[\sum_{\vec{R}} H_n(\alpha|\vec{\rho} - \vec{R}|) \exp(in\phi_{\vec{\rho}-\vec{R}}) \exp(ik_z z) \exp(i\vec{k}_\parallel \cdot \vec{R}) \right]$$

$$= \sum_g \frac{2(-i)^{n-1}}{a_1\sqrt{\alpha^2 - |\vec{k}_\parallel + \vec{g}|^2}} \exp(in\phi_{\vec{k}\alpha g}^\pm)(\vec{k}_{\alpha g}^\pm + k_z\hat{e}_z) \exp(i\vec{k}_{\alpha g}^\pm \cdot \vec{\rho}) \exp(ik_z z)$$

$$= \sum_g \vec{B}_{n1}^{g\pm} \exp(i\vec{k}_{\alpha g}^\pm \cdot \vec{\rho}) \exp(ik_z z), \tag{D.10}$$

where

$$\vec{B}_{n1}^{g\pm} = \frac{2(-i)^{n-1}}{a_1\sqrt{\alpha^2 - |\vec{k}_\parallel + \vec{g}|^2}} \exp(in\phi_{\vec{k}\alpha g}^\pm)(\vec{k}_{\alpha g}^\pm + k_z\hat{e}_z). \tag{D.11}$$

In the same way,

$$\sum_{\vec{R}} \exp(i\vec{k}_\parallel \cdot \vec{R}) \vec{H}_{n2}(\vec{r} - \vec{R})$$

$$= \sum_g \frac{2(-i)^{n-1}}{a_1\sqrt{\beta^2 - |\vec{k}_\parallel + \vec{g}|^2}} \exp(in\phi_{\vec{k}\beta g}^\pm)(\vec{k}_{\beta g}^\pm \times \hat{e}_z) \exp(i\vec{k}_{\beta g}^\pm \cdot \vec{\rho}) \exp(ik_z z)$$

$$= \sum_g \vec{B}_{n2}^{g\pm} \exp(i\vec{k}_{\beta g}^\pm \cdot \vec{\rho}) \exp(ik_z z), \tag{D.12}$$

where

$$\vec{B}_{n2}^{g\pm} = \frac{2(-i)^{n-1}}{a_1\sqrt{\beta^2 - |\vec{k}_\parallel + \vec{g}|^2}} \exp(in\phi_{\vec{k}\beta g}^\pm)(\vec{k}_{\beta g}^\pm \times \hat{e}_z). \tag{D.13}$$

Similarly,

$$\sum_{\vec{R}} \exp(i\vec{k}_\parallel \cdot \vec{R}) \vec{H}_{n3}(\vec{r} - \vec{R})$$

$$= \frac{1}{\beta} \nabla \times \sum_{\vec{R}} \exp(i\vec{k}_\parallel \cdot \vec{R}) \vec{H}_{n3}(\vec{r} - \vec{R})$$

$$= \sum_g \frac{2(-i)^{n-2}}{a_1\sqrt{\beta^2 - |\vec{k}_\parallel + \vec{g}|^2}} \exp(in\phi_{\vec{k}\beta g}^\pm) \left(\frac{k_z}{\beta}\vec{k}_{\beta g}^\pm - \beta\hat{e}_z \right) \exp(i\vec{k}_{\beta g}^\pm \cdot \vec{\rho}) \exp(ik_z z)$$

$$= \sum_g \vec{B}_{n3}^{g\pm} \exp(i\vec{k}_{\beta g}^\pm \cdot \vec{\rho}) \exp(ik_z z), \tag{D.14}$$

with

$$\vec{B}_{n3}^{g\pm} = \frac{2(-i)^{n-2}}{a_1\sqrt{\beta^2 - |\vec{k}_\parallel + \vec{g}|^2}} \exp(in\phi_{\vec{k}\beta g}^\pm) \left(\frac{k_z}{\beta}\vec{k}_{\beta g}^\pm - \beta\hat{e}_z \right). \tag{D.15}$$

References

[1] Yablonovitch E and Gmitter T J 1989 *Phys. Rev. Lett.* **63** 1950
[2] Ho K M, Chan C T and Soukoulis C M 1990 *Phys. Rev. Lett.* **65** 3152

[3] Sigalas M and Economou E N 1993 *Solid State Commun.* **86** 141
[4] Economou E N and Sigalas M 1994 *J. Acoust. Soc. Am.* **95** 1734
[5] Kushwaha M S, Halevi P and Martinez G 1994 *Phys. Rev.* B **49** 2313
[6] Montero de Espinosa F R, Jimenez E and Torres M 1998 *Phys. Rev. Lett.* **80** 1208
[7] Liu Z, Chan C T, Sheng P, Goertzen A L and Page J H 2000 *Phys. Rev.* B **62** 2446
[8] Mei J, Liu Z, Shi J and Tian D 2003 *Phys. Rev.* B **67** 245107
[9] Kafesaki M and Economou E N 1999 *Phys. Rev.* B **60** 11993
[10] Psarobas I E, Stefanou N and Modinos A 2000 *Phys. Rev.* B **62** 278
[11] Wilm W, Khelif A, Ballandras S, Laude V and Djafari-Rouhani B 2003 *Phys. Rev.* E **67** 065602
[12] Khelif A, Wilm M, Laude V, Ballandras S and Djafari-Rouhani B 2004 *Phys. Rev.* E **69** 067601
[13] Laude V, Khelif A, Benchabane S, Wilm M, Sylvestre T, Kibler B, Mussot A, Dudley J M and Maillotte H 2005 *Phys. Rev.* B **71** 045107
[14] Nicorovici N A and McPhedran R C 1994 *Phys. Rev.* E **49** 4563
[15] Pendry J B 1974 *Low Energy Electron Diffraction* (London: Academic)
[16] Goffaux C and Vigneron J P 2001 *Phys. Rev.* B **64** 075118
[17] Chew W C 1990 *Waves and Fields in Inhomogeneous Media* (New York: Van Nostrand-Reinhold)